Supplementary Information

Free-Standing *T*-Nb_2O_5/Graphene Composite Papers with Ultrahigh Gravimetric/Volumetric Capacitance for Li-Ion Intercalation Pseudocapacitor

Lingping Kong, Chuanfang Zhang, Jitong Wang, Wenming Qiao, Licheng Ling and Donghui Long*

State Key Laboratory of Chemical Engineering, East China University of Science and Technology, Shanghai 200237, China

* Corresponding author: Donghui Long, Tel: +86-21-64252924. Fax: +86-21-64252914.

E-mail: longdh@mail.ecust.edu.cn

Content:

Figure S1. TG analysis of Nb_2O_5/rGO and *T*-Nb_2O_5/graphene composite papers in air flow.

Figurs S2. CV curves of *T*-Nb_2O_5/graphene composite papers with the sweep rates ranging from 50-500 mV s^{-1}.

Figure S3. Nyquist plot ranging from 100 kHz to 0.01 Hz for *T*-Nb_2O_5/graphene (a) and Nb_2O_5/rGO (b) composite papers.

Figure S4. Rate capability (a) and cycling performance (b) of *T*-Nb_2O_5/graphene composite papers.

Figure S5. Top-view (a) and cross-sectional SEM image (b) of *T*-Nb_2O_5/graphene composite papers after 1700 charge-discharge tests at current density 1 A g^{-1}.

Figure S6. The k_1, k_2-value at different potential with the sweep rate ranging from 1-10 mV s^{-1} for *T*-Nb_2O_5/graphene composite papers.

Figure S7. Determination of the infinite sweep rate capacitance of *T*-Nb_2O_5/graphene composite papers.

Figure S8. Mass ratio of AC and *T*-Nb_2O_5/graphene papers is 6.5 (a) and 3.5 (b).

Table S1. Characteristics of Nb_2O_5/rGO and *T*-Nb_2O_5/graphene composite papers.

Table S2. Porosity parameters of Nb_2O_5/rGO and *T*-Nb_2O_5/graphene composite papers.

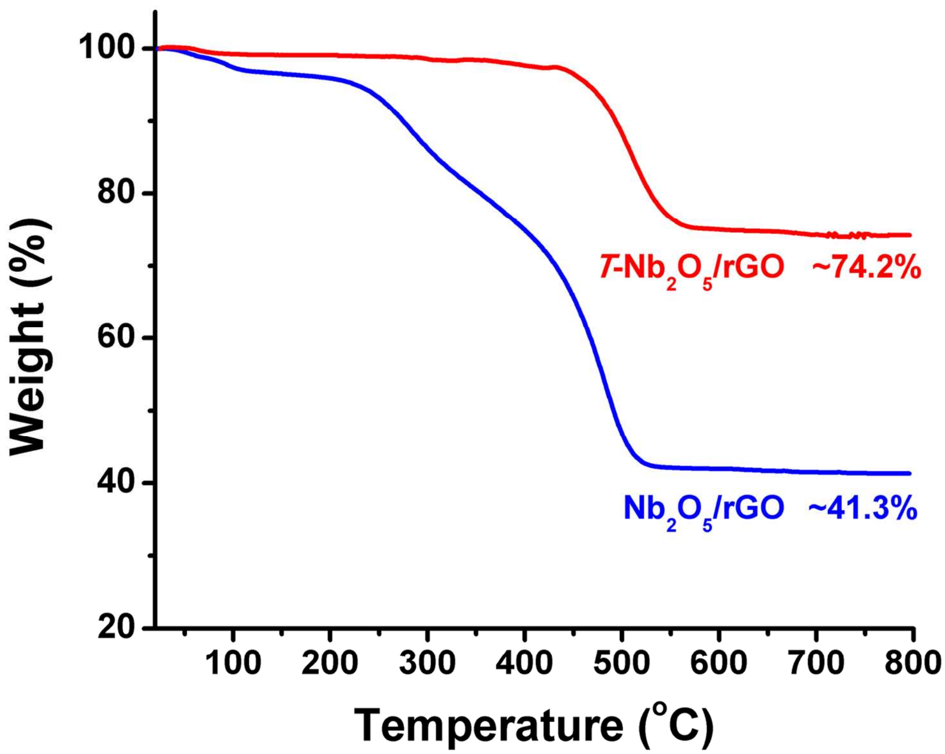

Figure S1. TG analysis of Nb_2O_5/rGO and *T*-Nb_2O_5/graphene composite papers in air flow.

Nb_2O_5/rGO composite paper had a slight weight loss before around 230 ^{o}C corresponding to the loss of free water and bound water, then had a linear weight loss between 250 ~ 450 ^{o}C due to the decomposition of oxygen functional groups in graphite oxide (GO). After about 450 ^{o}C, Nb_2O_5/rGO and *T*-Nb_2O_5/graphene composite papers had a decimated weight loss, corresponding to the combustion of carbon. The weight content of Nb_2O_5 in Nb_2O_5/rGO and *T*-Nb_2O_5/graphene composite papers was calculated to be 41.3 wt. % and 74.2 wt. %, respectively.

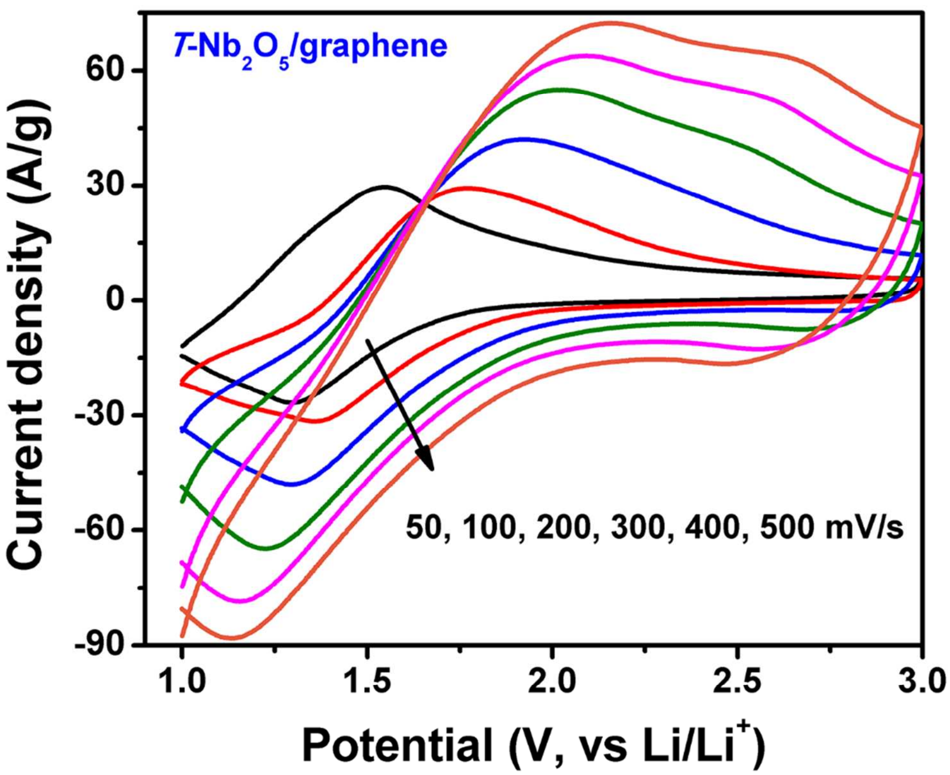

Figurs S2. CV curves of *T*-Nb_2O_5/graphene composite papers with the sweep rates ranging from 50-500 mV s^{-1}.

As the sweep rate increasing, the cathodic and anodic current peaks shift significantly, which should be attributed to the diffusion-controlled ohmic contributions.

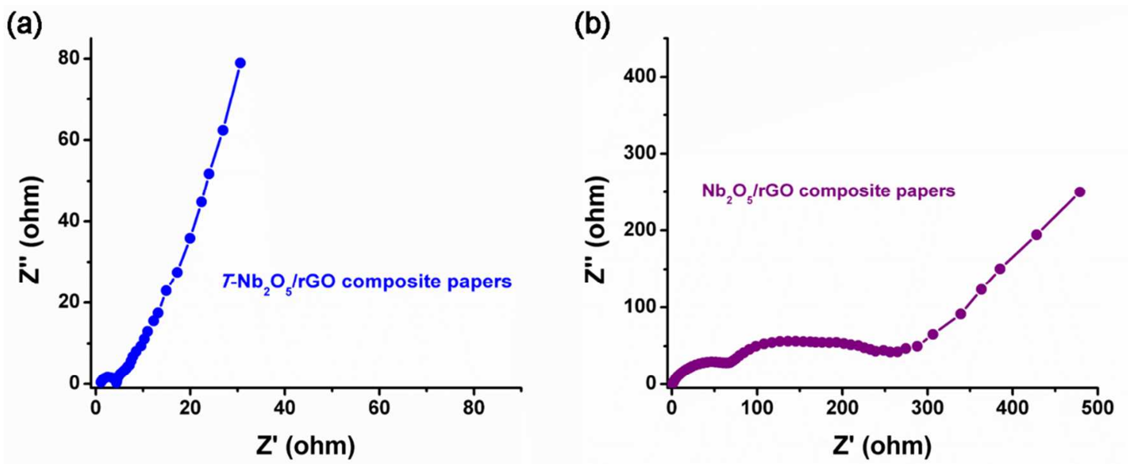

Figure S3. Nyquist plot ranging from 100 kHz to 0.01 Hz for *T*-Nb_2O_5/graphene (a) and Nb_2O_5/rGO (b) composite papers.

A lower faradic charge transfer resistance for *T*-Nb_2O_5/graphene composite papers, indicated fast Li^+ intercalation redox reaction occurred. The low charge transfer resistance can be attributed to the electron transport highways built up from the layer by layer network, and the sheet-like channel among the assembled papers is favorable used as reservoir for electrolyte ions.

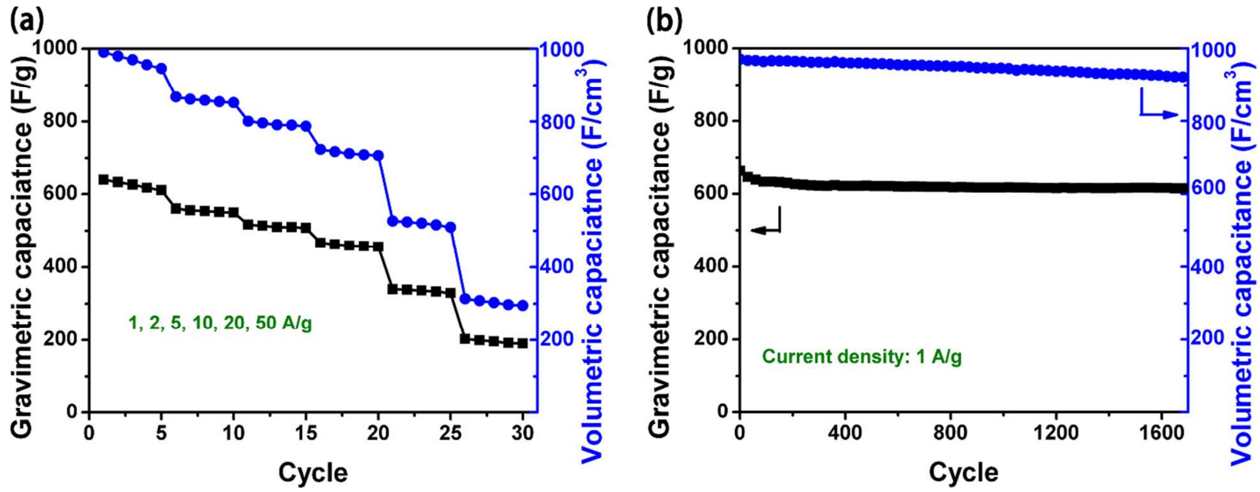

Figure S4. Rate capability (a) and cycling performance (b) of *T*-Nb_2O_5/graphene composite papers.

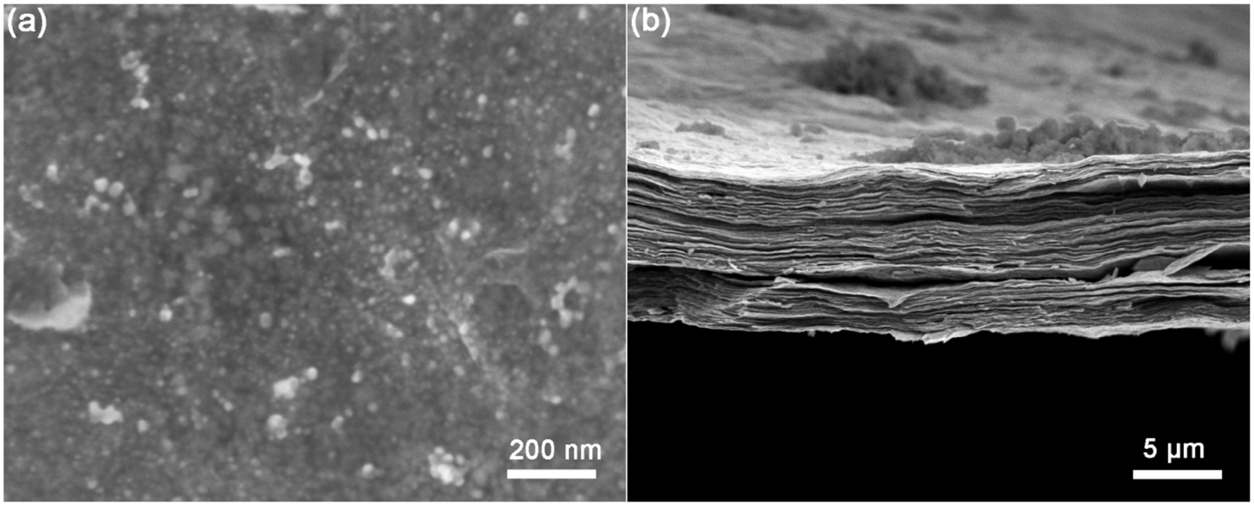

Figure S5. Top-view (a) and cross-sectional SEM image (b) of *T*-Nb_2O_5/graphene composite papers after 1700 charge-discharge tests at current density 1 A g^{-1}.

After 1700 charge-discharge cycling, the layer stacked structure of *T*-Nb_2O_5/graphene composite papers could maintain and *T*-Nb_2O_5 nanoparticles still tightly anchor on the graphene surface, confirming the structural advantages of free-standing *T*-Nb_2O_5/graphene composite papers in keeping the structural stability and integrity.

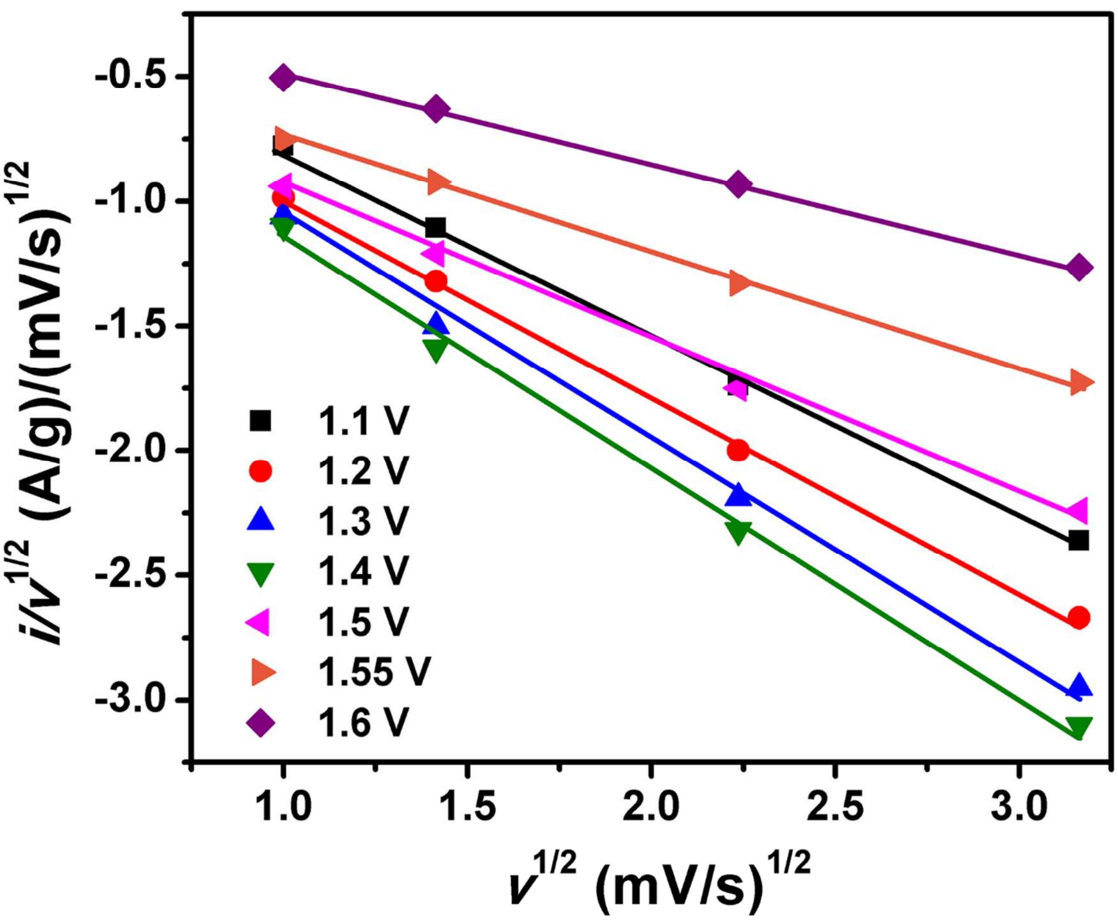

Figure S6. The k_1, k_2-value at different potential with the sweep rate ranging from 1-10 mV s^{-1} for *T*-Nb_2O_5/graphene composite papers.

The equation (2) can be rearranged to equation $i(V)/v^{1/2} = k_1 v^{1/2} + k_2$. Thus, the value of k_1 and k_2-value can be determined by plotting $v^{1/2}$ vs $i/v^{1/2}$ and k_1 and k_2 are constant at the fixed potential.

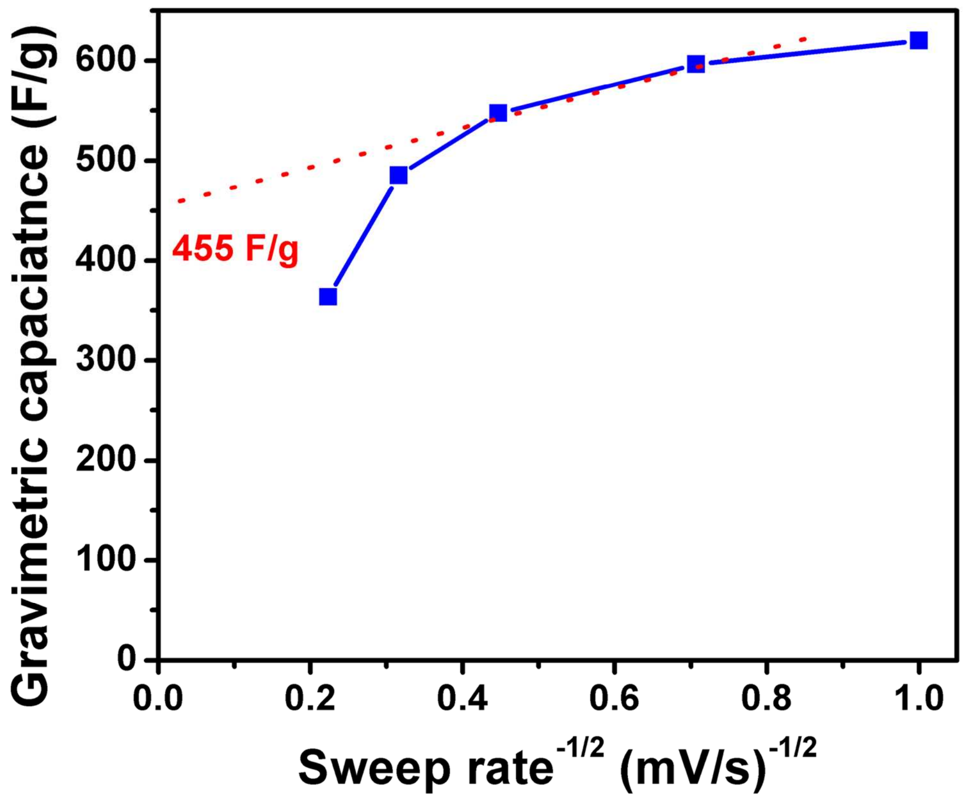

Figure S7. Determination of the infinite sweep rate capacitance of *T*-Nb_2O_5/graphene composite papers.

By rewriting the equation (3), the following relationship arises:

$Q(v) = Q_{\text{capacitive}} + \text{constant}(v^{-1/2})$

By plotting capacitance vs. $v^{-1/2}$ yields a straight line whose y-intercept ($v = \infty$) is the infinite-sweep rate capacitance. Due to the polarization effect at high sweep rates, deviation from a straight line usually occurs, and intermediate sweep rates are then selected to extrapolate to the y-intercept.

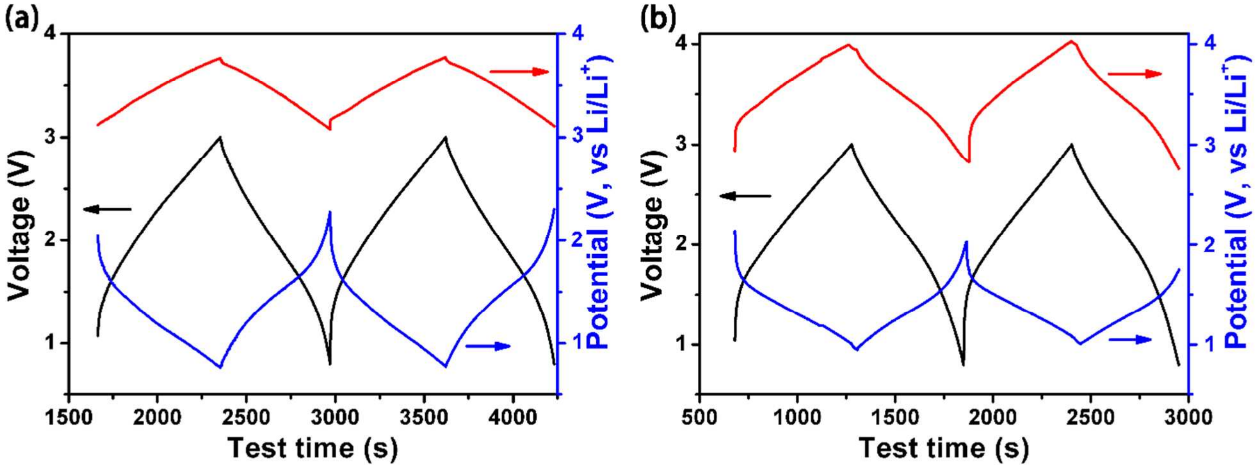

Figure S8. Mass ratio of AC and T-Nb_2O_5/graphene papers is 6.5 (a) and 3.5 (b).

The specific capacitance of each electrode was calculated from the discharge curves. The optimal mass ratio between the positive and negative electrodes would be obtained, when the charge (q) strikes balance across the two electrodes ($q_+ = q_-$). The charge stored by each electrode usually depends on the specific capacitance (C), the work operating voltage (ΔE) and the mass of the electrode (m) following equation:

$q = C \times \Delta E \times m$

By the formula conversion, the mass ratio of two electrodes should follow:

$m_+/m_- = (C_- \times \Delta E_-)/(C_+ \times \Delta E_+)$

The asymmetric supercapacitors were charged and discharged at 0.5 A g^{-1} with the different mass ratio of positive and negative electrodes. Through the formula of $m_+/m_- = (C_- \times \Delta E_-)/(C_+ \times \Delta E_+)$, the optimal mass ratio of AC and T-Nb_2O_5/graphene papers is calculated and has been chosen as 3.5.

Table S1. Porosity parameters of Nb_2O_5/rGO and *T*-Nb_2O_5/graphene composite papers.

Samples	[a] $\mathbf{S_{BET}}$ [$\mathbf{m^2\ g^{-1}}$]	[b] $\mathbf{V_T}$ [$\mathbf{cm^3\ g^{-1}}$]	[c] $\mathbf{D_{ave}}$ **[nm]**
$\mathbf{Nb_2O_5}$/rGO	285.3	0.156	-
***T*-$\mathbf{Nb_2O_5}$/rGO**	209.6	0.263	5.0

[a] BET specific surface area; [b] total pore volume; [c] BJH average pore diameter from desorption branch

Table S2. Characteristics of Nb_2O_5/rGO and *T*-Nb_2O_5/graphene composite papers.

Sample	**Thickness [μm]**	**Density [g $\mathbf{cm^{-3}}$]**	**resistivity [S $\mathbf{cm^{-1}}$]**
$\mathbf{Nb_2O_5}$/rGO	22	0.81	0.12
***T*-$\mathbf{Nb_2O_5}$/rGO**	11	1.55	2.5